

# UC Irvine

## UC Irvine Previously Published Works

### Title

Characterization of fluid flow velocity by optical Doppler tomography.

### Permalink

<https://escholarship.org/uc/item/2c79320k>

### Journal

Optics Letters, 20(11)

### ISSN

0146-9592

### Authors

Wang, XJ  
Milner, TE  
Nelson, JS

### Publication Date

1995-06-01

### DOI

10.1364/ol.20.001337

### Copyright Information

This work is made available under the terms of a Creative Commons Attribution License, available at <https://creativecommons.org/licenses/by/4.0/>

Peer reviewed

# Characterization of fluid flow velocity by optical Doppler tomography

X. J. Wang, T. E. Milner, and J. S. Nelson

Beckman Laser Institute and Medical Clinic Departments of Surgery and Dermatology, University of California, Irvine, Irvine, California 92715

Received December 19, 1994

The spatial profiles of fluid flow velocity in transparent glass and turbid collagen conduits are measured by optical Doppler tomography (ODT). The flow velocity at a discrete user-specified spatial location in the conduit is determined by measurement of the Doppler shift of backscattered light from microspheres suspended in the flowing fluid. Experimental data and theoretical calculations are in excellent agreement. ODT is an accurate method for the characterization of high-resolution fluid flow velocity.

Optical low-coherence reflectometry (OLCR) is a non-contact technique used in tomographic imaging<sup>1-3</sup> and nondestructive testing<sup>4-6</sup> of static structures. OLCR determines the location and relative strength of optically scattering structures by measuring the interference fringe intensity of light backscattered from a test material. The method has high sensitivity (e.g., >140-dB dynamic range) and exceptional spatial resolution (1–10  $\mu\text{m}$ ) in the axial and radial directions. In this Letter we report the use of OLCR in combination with the Doppler effect to measure spatial profiles of fluid flow velocity in transparent glass and turbid collagen conduits.

Light emitted from a He–Ne laser ( $\lambda_0 = 632.8 \text{ nm}$ ) and a superluminescent diode (SLD) is coupled into a fiber-optic Michelson interferometer with a  $2 \times 1$  coupler. He–Ne light serves only as an aiming beam and is blocked during fluid flow measurement. SLD light ( $\lambda_0 = 632.8 \text{ nm}$ ,  $P_0 = 1 \text{ mW}$ ) is split into reference and test beams by a  $2 \times 2$  (50:50) fiber coupler (Fig. 1). Light intensity in the reference arm is attenuated to  $2 \mu\text{W}$  to yield a higher signal-to-noise ratio.<sup>7</sup> The optical phase in the reference and test arms is modulated (1000 Hz) with piezoelectric cylinders driven by a serrodyne (i.e., ramp) waveform. Stress birefringence is used to match the polarity of the beams and optimize fringe contrast.

Light in the target arm is focused into a test conduit carrying a flowing fluid that contains polymer microspheres (diameter  $2.062 \pm 0.025 \mu\text{m}$ ) suspended in distilled and doubly deionized water (concentration  $c = 3.4 \times 10^7 \text{ cm}^{-3}$ ) forced through the conduit by a linear syringe pump. Light that is Doppler shifted and backscattered from the microspheres within the conduit and from the reference mirror recombines within the  $2 \times 2$  coupler and interferes only when the path length difference is less than or equal to the coherence length of the SLD source light. Power spectra of the optical interference fringe intensity are measured by a photoreceiver (New Focus 2001) in combination with a spectrum analyzer (HP 8560E). Because the coherence envelope of SLD source light yields rapid phase decorrelation of the target and reference beams for path length differences greater than the coherence length,<sup>8</sup> high spatial resolution ( $<10 \mu\text{m}$ ) is achieved.

Optical interference fringe intensities are recorded of light backscattered from a transparent glass conduit of square cross section ( $500 \mu\text{m} \times 500 \mu\text{m}$ ) containing stationary and flowing microspheres (Fig. 2). The recorded scans represent the optical interference intensity of light backscattered from positions along a line passing through the center of the conduit and perpendicular to the walls. Four principal peaks observed in both traces represent reflections from the glass walls of the conduit (from left to right: air–glass, glass–fluid, fluid–glass, and glass–air). In the case of stationary microspheres, the fringe intensity inside the conduit shows little variation with position. When microspheres are flowing, fringe intensity is reduced in regions of greater flow velocity, because light backscattered from inside the conduit is Doppler shifted out of the sensitive bandwidth of the spectrum analyzer (i.e.,  $1000 \pm 15 \text{ Hz}$ ). The measured fringe intensity is greater at regions near the conduit wall because the Doppler shift of backscattered light is smaller. Inasmuch as the horizontal axis (Fig. 2) represents the scanning position in air, the inner dimension of the glass conduit ( $D$ ) is

$$D = T \sin(\phi')/n_g, \quad (1)$$

where  $T$  is the measured optical path length inside the conduit,  $\phi'$  is the tilt angle between the direction of light propagation in the conduit and the flow stream, and  $n_g$  is the group refractive index of the flowing fluid.

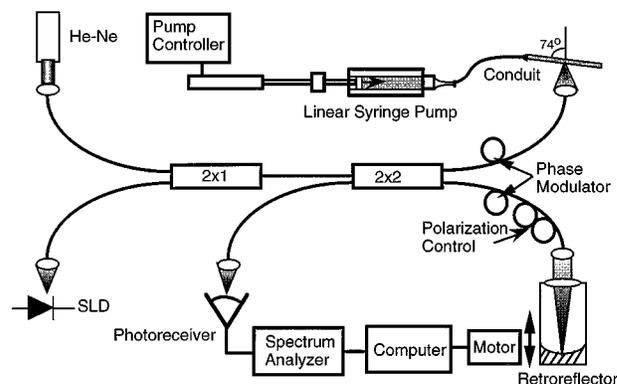


Fig. 1. Schematic of ODT instrumentation.

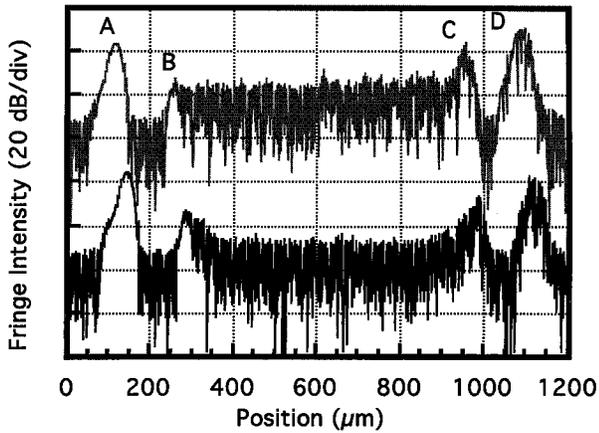


Fig. 2. OLCR scans of static (upper curve) and flowing (lower curve) microspheres suspended in a glass conduit (curves offset by 60 dB). The four principal peaks (air-glass, glass-fluid, fluid-glass, and glass-air) are labeled A, B, C, and D, respectively.

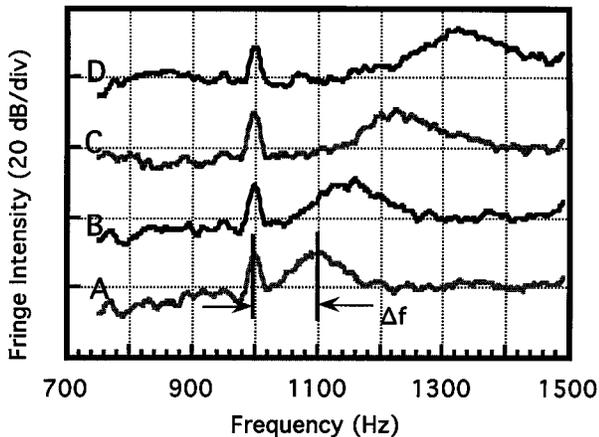


Fig. 3. Power spectra of four flow velocities (A, 188; B, 287; C, 423; D, 620  $\mu\text{m/s}$ ) at a discrete spatial location in a glass conduit (curves offset by 20 dB).

Because optical dispersion is small (i.e.,  $dn/d\lambda \approx 0$ ),  $n_g$  is approximated by the refractive index  $n$ . We measure  $T = 690 \mu\text{m}$ ,  $\phi' = 78.0^\circ$ , and  $n(\lambda = 850 \text{ nm}) = 1.329$ , to find  $D = 508 \pm 4 \mu\text{m}$ , consistent with the manufacturer's specified value ( $D = 500 \pm 5 \mu\text{m}$ ).

To detect the Doppler-shifted signal, we tilt the optical axis of the target arm relative to the flow direction to give a component of the velocity parallel to the incoming light propagation vector. Power spectra of the optical interference fringe intensity are measured for backscattered light from a single position within the glass conduit at four increasing flow velocities (Fig. 3). Narrow and broad peaks in each trace represent, respectively, the base modulation (1000 Hz) and the Doppler-shifted frequencies from the flowing microspheres. A sharper velocity gradient at greater fluid flow velocity contributes to increased Doppler broadening.

Centroid measurement of the Doppler-shifted spectrum  $[\Delta f(x)]$  at each position in the conduit permits determination of the velocity profile  $[V(x)]$  of the flowing fluid,

$$V(x) = \Delta f(x) \lambda_0 / 2 \cos(\phi'), \quad (2)$$

where  $\lambda_0 = 850 \text{ nm}$  is the vacuum center wavelength of SLD emission. Including corrections for  $\phi'$  and  $n$ , the flow velocity profile is measured over a central axis  $[V(x, y = D/2)]$  in the glass conduit (Fig. 4). The velocity distribution in the conduit is computed by applying Poiseuille's model<sup>9</sup> and solving the Navier-Stokes equation<sup>10</sup> with a nonslip boundary condition at the fluid-glass interface  $[V(x, y = 0 \text{ or } D) = 0 \text{ and } V(x = 0 \text{ or } D, y = 0)]$ . For the model, the velocity profile through the central cross section is expressed as a Fourier series,

$$V(x, y = D/2) = \frac{16D^2\Delta p}{\pi^4\mu\Delta L} \times \sum_{n=2i+1} \sum_{m=2j+1} \frac{\sin(n\pi/2)\sin(m\pi x/D)}{mn(n^2 + m^2)}, \quad i, j = 0, 1, 2, 3 \dots, \quad (3)$$

where  $\Delta p$  is the pressure difference along a length,  $\Delta L$ , of the conduit and  $\mu$  is dynamic viscosity of the flowing fluid. Inasmuch as the Reynolds number is less than unity in our experiments, laminar flow is expected,<sup>9</sup> and the flow velocity diminishes monotonically with increased distance from the central axis of the conduit. We deduce a theoretical fit to the experimental data (Fig. 4) by taking  $\Delta p/\Delta L$  as a fitting parameter. Average flow velocity over a central axis, determined from the experimental data ( $217 \pm 6 \mu\text{m/s}$ ), compares well with that computed ( $212 \mu\text{m/s}$ ) from the flow rate.

To investigate the potential application of ODT for measuring fluid flow embedded in scattering media, we measured velocity profiles within a turbid cylindrical collagen conduit. The collagen wall represents an optical scattering barrier similar to that found in tissue. For laminar flow, the velocity distribution  $[V(r)]$  in a cylindrical conduit at radial position  $r$  is

$$V(r) = \frac{d^2\Delta p}{16\mu\Delta L} \left[ 1 - \left( \frac{2r}{d} \right)^2 \right]. \quad (4)$$

Circular symmetry results in the development of a parabolic velocity flow profile in the cylindrical conduit. The inner diameter ( $d = 940 \mu\text{m}$ ) and the wall thickness ( $210 \mu\text{m}$ ) of the cylindrical collagen conduit are determined from an OLCR scan [Eq. (1)]. Velocity

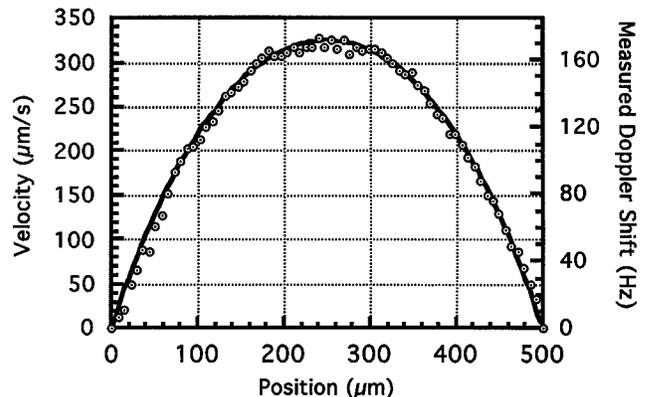


Fig. 4. Experimental (circles) and theoretical (solid curve) velocity profiles and corresponding Doppler shifts in a glass conduit of square cross section (velocity uncertainty  $\Delta V/V = 3\%$ ).

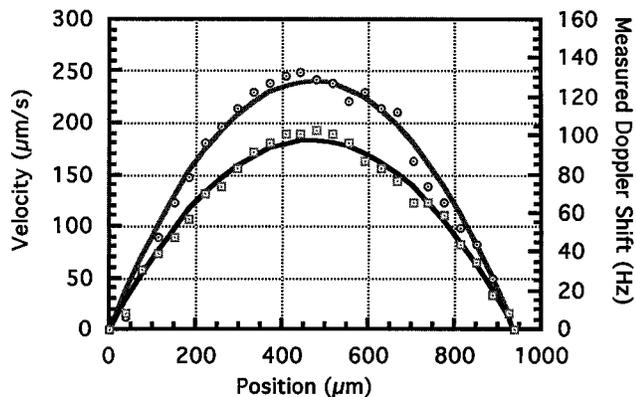


Fig. 5. Experimental (circles and squares) and theoretical (solid curves) velocity profiles in a turbid cylindrical collagen conduit of inner diameter  $d = 940 \mu\text{m}$  (velocity uncertainty  $\Delta V/V = 7\%$ ).

profiles corresponding to two pump speeds are measured across a central diameter of the collagen conduit. Theoretical fits [Eq. (4)] for both velocity profiles are in excellent agreement with measured values (Fig. 5).

ODT may provide useful information for applications that require knowledge of the presence of the flow of blood or other fluids at discrete spatial locations within tissue. Within the past decade, many researchers have investigated the application of noninvasive optical techniques such as laser Doppler flowmetry to study fluid flow.<sup>11</sup> Because such methods use coherent light sources, spatial resolution is compromised, and one cannot detect the flow velocity at a discrete user-specified spatial location within an individual conduit embedded in a highly scattering medium. Multigated ultrasound Doppler imaging<sup>12</sup> can resolve flow velocities at different positions; axial resolution, however, is 10 times coarser than that reported here. Moreover, in the acoustic case, the mean Doppler frequency is affected by many factors and may be more difficult to interpret.<sup>13</sup> Proper application of ODT permits accurate measurement of the fluid flow velocity profile with excellent spatial resolution. Furthermore, because hardware requirements are relatively simple, the use of ODT for biomedical applications such as blood flow monitoring are under investigation in our laboratory

The authors thank Howard Nathel, Lars Svaasand, and Wayne Sorin for helpful discussions and Wen Wang and Michael Chang for technical assistance. This project is supported through an academic equipment grant from Hewlett-Packard Laboratories and a post-doctoral fellowship to X. J. Wang and Independent Research Grants to J. S. Nelson and T. E. Milner from National Institutes of Health. Institute support from Office of Naval Research, U.S. Department of Energy, and National Institutes of Health is also gratefully acknowledged.

## References

1. X. Clivaz, F. Marquis-Weible, R. P. Salathé, R. P. Novák, and H. H. Gilgen, *Opt. Lett.* **17**, 4 (1992).
2. D. Huang, E. A. Swanson, C. P. Lin, J. S. Schuman, W. G. Stinson, W. Chang, M. R. Hee, T. Flotte, K. Gregory, C. Puliafato, and J. G. Fujimoto, *Science* **254**, 1178 (1991).
3. J. M. Schmitt, A. Knüttel, and R. F. Bonner, *Appl. Opt.* **32**, 6032 (1993).
4. X. J. Wang, T. E. Milner, R. P. Dhond, W. V. Sorin, S. A. Newton, and J. S. Nelson, *Opt. Lett.* **20**, 524 (1995).
5. W. V. Sorin and D. F. Gray, *IEEE Photon. Technol. Lett.* **4**, 105 (1992).
6. M. R. Hee, D. Huang, E. A. Swanson, and J. G. Fujimoto, *J. Opt. Soc. Am. B* **9**, 903 (1992).
7. W. V. Sorin and D. M. Baney, *IEEE Photon. Technol. Lett.* **4**, 1404 (1992).
8. J. W. Goodman, *Statistical Optics* (Wiley, New York, 1985), p.157.
9. L. D. Landau and E. M. Lifshitz, *Fluid Mechanics*, 2nd ed. (Pergamon, Oxford, 1987), Chap. 2, pp. 52–57.
10. M. Spiga and G. L. Morini, *Int. Commun. Heat Mass Transf.* **21**, 469 (1994).
11. R. F. Bonner and R. Nossal, in *Laser-Doppler Blood Flowmetry*, A. P. Shepherd and P. A. Öberg, eds. (Kluwer, Dordrecht, The Netherlands, 1990), Chap. 2, p. 17.
12. J. V. Chapman, in *The Noninvasive Evaluation of Hemodynamics in Congenital Heart Disease*, J. V. Chapman and G. R. Sutherland, eds. (Kluwer, Dordrecht, The Netherlands, 1990), Chap. 2, p. 57.
13. P. A. J. Bascom and R. S. C. Cobbold, *Ultrasound Med. Biol.* **16**, 279 (1990).